



The Atypical Cadherin Dachshous Controls Left-Right Asymmetry in *Drosophila*.

Nicanor González-Morales, Charles Gémard, Gaëlle Lebreton, Delphine Cerezo, Jean-Baptiste Coutelis, Stéphane Noselli

► To cite this version:

Nicanor González-Morales, Charles Gémard, Gaëlle Lebreton, Delphine Cerezo, Jean-Baptiste Coutelis, et al.. The Atypical Cadherin Dachshous Controls Left-Right Asymmetry in *Drosophila*.. *Developmental Cell*, 2015, 33 (6), pp.675-89. 10.1016/j.devcel.2015.04.026 . hal-01254733

HAL Id: hal-01254733

<https://hal.science/hal-01254733>

Submitted on 10 Feb 2021

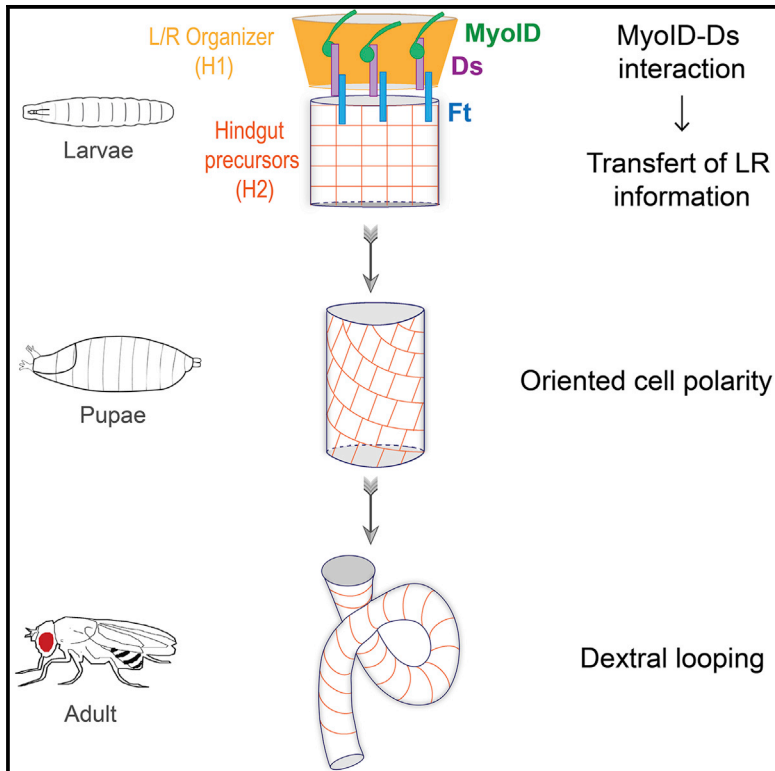
HAL is a multi-disciplinary open access archive for the deposit and dissemination of scientific research documents, whether they are published or not. The documents may come from teaching and research institutions in France or abroad, or from public or private research centers.

L'archive ouverte pluridisciplinaire **HAL**, est destinée au dépôt et à la diffusion de documents scientifiques de niveau recherche, publiés ou non, émanant des établissements d'enseignement et de recherche français ou étrangers, des laboratoires publics ou privés.

Developmental Cell

The Atypical Cadherin Dachsous Controls Left-Right Asymmetry in *Drosophila*

Graphical Abstract



Authors

Nicanor González-Morales, Charles Gémard, Gaëlle Lebreton, Delphine Cerezo, Jean-Baptiste Coutelis, Stéphane Noselli

Correspondence

noselli@unice.fr

In Brief

Myosin ID (myoID) controls left-right (LR) asymmetry in *Drosophila*. González-Morales et al. show that MyoID interacts with the intracellular domain of the atypical cadherin Dachsous (Ds) in a tissue-specific LR organizer, suggesting that MyoID-Ds interaction propagates LR information from the organizer to precursor tissues essential for asymmetric organ development.

Highlights

- Myosin ID (MyoID) controls hindgut left-right (LR) asymmetry and dextral looping
- *Drosophila* atypical cadherin Dachsous (Ds) is essential for hindgut LR asymmetry
- MyoID interacts with Ds intracellular domain for proper LR asymmetry
- Ds propagates MyoID LR information from LR organizer to hindgut precursors



The Atypical Cadherin Dachsous Controls Left-Right Asymmetry in *Drosophila*

Nicanor González-Morales,^{1,2,3} Charles Géminard,^{1,2,3} Gaëlle Lebreton,^{1,2,3} Delphine Cerezo,^{1,2,3} Jean-Baptiste Coutelis,^{1,2,3} and Stéphane Noselli^{1,2,3,*}

¹Institut de Biologie Valrose, University of Nice Sophia Antipolis, 06108 Nice, France

²Institut de Biologie Valrose, CNRS, UMR 7277, 06108 Nice, France

³Institut de Biologie Valrose, INSERM, U1091, 06108 Nice, France

*Correspondence: noselli@unice.fr

<http://dx.doi.org/10.1016/j.devcel.2015.04.026>

SUMMARY

Left-right (LR) asymmetry is essential for organ development and function in metazoans, but how initial LR cue is relayed to tissues still remains unclear. Here, we propose a mechanism by which the *Drosophila* LR determinant Myosin ID (MyoID) transfers LR information to neighboring cells through the planar cell polarity (PCP) atypical cadherin Dachsous (Ds). Molecular interaction between MyoID and Ds in a specific LR organizer controls dextral cell polarity of adjoining hindgut progenitors and is required for organ looping in adults. Loss of Ds blocks hindgut tissue polarization and looping, indicating that Ds is a crucial factor for both LR cue transmission and asymmetric morphogenesis. We further show that the Ds/Fat and Frizzled PCP pathways are required for the spreading of LR asymmetry throughout the hindgut progenitor tissue. These results identify a direct functional coupling between the LR determinant MyoID and PCP, essential for non-autonomous propagation of early LR asymmetry.

INTRODUCTION

Left-right (LR) asymmetry is a prominent feature of bilateria (for a recent review, see Blum et al., 2014; Coutelis et al., 2014; Nakamura and Hamada, 2012; Namigai et al., 2014; Vandenberg and Levin, 2013; Yoshida and Hamada, 2014). Differentiating two body sides is essential for positioning organs, controlling their looping and, ultimately, their function. Abnormalities in LR patterning can lead to a range of defects, including loss of asymmetry (isomerism), loss of concordance between organs (heterotaxia, situs ambiguous), and inversion of the LR axis (situs inversus); several congenital health-threatening or lethal conditions are indeed linked to defects in LR asymmetry (Peeters and Devriendt, 2006). Understanding how symmetry is initially broken and how de novo asymmetry is transferred to tissues during development yields major questions. Studies using a range of vertebrate model organisms have revealed some original patterning mechanisms, including the generation of ion flux in pre-gastrula embryos, the generation of a leftward flow at the

embryonic node through rotating cilia, and asymmetrical cell movement (Adams et al., 2006; Blum et al., 2014; Coutelis et al., 2014; Cui et al., 2009; Gros et al., 2009; Lenhart et al., 2013; Levin et al., 2002; Namigai et al., 2014; Vandenberg and Levin, 2013; Yoshida and Hamada, 2014). These early events contribute to symmetry breaking, ultimately leading to asymmetric activation of the conserved nodal/transforming growth factor β (TGF- β) pathway, which then controls organ asymmetrical morphogenesis (Raya and Izpisua Belmonte, 2006).

In contrast to vertebrates, *Drosophila* LR markers are relatively simple and homogeneous as they are restrained to tubular organs that undergo dextral morphogenesis; these include male terminalia rotation, looping of the larval and adult gut, and testis (Hozumi et al., 2006; Géminard et al., 2014; Spéder et al., 2006; Coutelis et al., 2008). Genes controlling LR asymmetry in flies have only recently been identified. The conserved type II myosin gene (*myosin ID*, *myoID*; also known as *myo31DF*) (Mooseker and Cheney, 1995; Morgan et al., 1995) is unique, as *myoID* loss of function leads to complete situs inversus with all asymmetric organs developing as sinistral (Hozumi et al., 2006; Géminard et al., 2014; Spéder et al., 2006; Coutelis et al., 2008). The expression of *myoID*—and, hence, LR symmetry breaking—is under the direct control of the HOX transcription factor Abdominal-B (Coutelis et al., 2013). It is interesting that tissue-targeted invalidation of *myoID* in the genital disc has revealed the existence of a restricted domain controlling dextral terminalia rotation, termed the “terminalia LR organizer” (Spéder et al., 2006). Knockdown of *myoID* in this specific terminalia LR organizer inverts the rotation of the terminalia; other organs, however, develop normally, suggesting the existence of additional tissue-specific LR organizers that remain to be characterized.

Planar cell polarity (PCP) is a global process coordinating cell behaviors in the plane of a tissue (Gray et al., 2011; Wallingford, 2012; for recent reviews, see Yang, 2012). In *Drosophila*, PCP is involved in the polarity of hair-like structures in many organs, including the wing, eye, abdomen, and notum (Adler, 2012; Lawrence et al., 2007; Lawrence and Casal, 2013; Matis and Axelrod, 2013; Singh and Mlodzik, 2012). The well-studied *Drosophila* PCP genes are known to belong to two major pathways: the “core system” and the “global system” (Axelrod, 2009; Goodrich and Strutt, 2011; Lawrence and Casal, 2013; Matis and Axelrod, 2013). The core system comprises the distally located (relative to the anterior-posterior [AP] axis of the wing, in addition to their polarity along the AP axis in other cell types) proteins Frizzled (Fz), Dishevelled (Dsh), and Diego (Dgo); the proximally

located proteins Van Gogh (Vang, aka Strabismus) and Prickle (Pk); and symmetrically localized Flamingo (Vinson and Adler, 1987; Krasnow et al., 1995; (Tree et al., 2002; Wolff and Rubin, 1998; Bastock et al., 2003; Das et al., 2002). The global system includes the atypical cadherins Fat (Ft) and Dachsous (Ds) and the Golgi kinase Four-Jointed (Fj) (Sharma and McNeill, 2013; Simon et al., 2010; Thomas and Strutt, 2012; Yang et al., 2002). Both systems rely on extracellular protein interactions and feedback signaling to ensure proper polarization of tissues (Axelrod, 2009; Goodrich and Strutt, 2011; Peng and Axelrod, 2012). Current studies suggest that the two pathways can interact in different ways, depending on the cell context, with Ds gradient direction and core module polarization oriented either parallel or anti-parallel (Zeidler et al., 2000; Casal et al., 2002; Ma et al., 2003; Matakatsu and Blair, 2004; Rogulja et al., 2008). Notably, it has been proposed that the global system provides a directionality cue that is then used by the core system to align the polarity of each cell with that of their neighbors (Hogan et al., 2011; Ma et al., 2003; Olofsson et al., 2014; Ayukawa et al., 2014).

The first hint of a role of PCP in LR asymmetry initially came from the identification of the mouse *inversin* gene (a distant homolog of the *diego* core-PCP gene), mutations of which lead to a high percentage of situs inversus (Morgan et al., 1998). More recently, the mouse PCP core pathway has been shown to control cilia positioning in the embryonic node, which is important for nodal flow and correct LR asymmetry (Antic et al., 2010; Song et al., 2010). However, so far, no study has linked global PCP and LR asymmetry.

In this study, we characterize a role of both core and global PCP pathways in *Drosophila* adult hindgut LR asymmetry downstream of MyoID. We identified the hindgut imaginal ring subdomain H1 as the LR organizer controlling the directional looping of the adult hindgut. In H1 cells, MyoID physically interacts with the intracellular domain of Ds to dextrally polarize cells from the H2 domain, corresponding to hindgut precursor cells. Polarization is inverted (sinistral) in *myoID* loss of function, while it is absent when *ds* is specifically invalidated in the H1 domain. In addition, *myoID* and *ds* interact genetically to polarize the H2 cells. Therefore, Ds is essential to convey MyoID-dependent LR information to neighboring H2 hindgut precursors. We further show that spreading of LR polarity within H2 precursor cells depends on both global and core PCP pathways. Thus, these results reveal a mechanism allowing cell-non-autonomous transmission of symmetry-breaking information from an LR organizer to organ precursors essential for proper LR morphogenesis.

RESULTS

MyoID Controls Directional Looping of the Adult Hindgut through a Specific LR Organizer

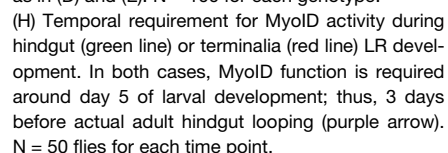
The *Drosophila* adult hindgut represents an attractive yet uncharacterized model for the study of MyoID-dependent control of de novo LR asymmetry. Indeed, adult hindgut LR asymmetry is established independently of larval hindgut asymmetry, as it derives from dedicated precursor cells clustered in the larval imaginal ring. The imaginal ring comprises two subdomains (H1 and H2), which are thought to give rise to the adult

sphincter-like pylorus, the absorptive ileum, and the stem cell region (Takashima et al., 2008, 2013; Fox and Spradling, 2009). During pupal development, imaginal ring derivatives proliferate and differentiate, while larvae counterparts degenerate (Robertson, 1936; Fox and Spradling, 2009). Thus, the transition from larval to adult hindgut provides an interesting model to characterize the mechanisms responsible for asymmetry cue transmission downstream of MyoID.

In wild-type flies, the adult hindgut coils clockwise, forming a single stereotyped loop localized on the right side of the abdomen when viewed dorsally (Figures 1A and 1D). Looping can be visualized by transmission microscopy using a non-invasive “blue feeding” method, which stains the gut lumen while keeping organs in their native configuration. The phenotype can be further analyzed by dissecting the whole fly abdomen, followed by confocal microscopy. Using these methods, we show that, in *myoID* null mutants, the adult hindgut displays an inverted sinistral phenotype in 80% of individuals (Figures 1B, 1E, and 1G); the remaining 20% of the population show a twisted phenotype, whereby the adult hindgut does not form a loop but a roughly symmetrical “S” shape (Figures 1C, 1F, and 1G). This phenotype can be reproduced when expressing *myoID-RNAi* driven either by *myoID-Gal4*, which mimics the *myoID* expression pattern (Figure 1G) (Coutelis et al., 2013; Petzoldt et al., 2012; Spéder et al., 2006), or *byn-Gal4* (hereinafter referred to as *hindgut-GAL4*), which is expressed in hindgut precursor cells (Figure 1G). Altogether, these observations show that, as in other LR organs, MyoID is required for the directionality of adult hindgut looping toward dextral (Hozumi et al., 2006).

At the posterior end of the adult hindgut is the rectum, which is part of the rotated terminalia but derives from both the genital disc and rectal larval cells (Fox et al., 2010). As *myoID* expression in the genital disc A8 segment controls dextral rotation of the terminalia, we asked whether *myoID* activity in the genital disc and/or rotation of the terminalia itself might be involved in adult hindgut looping. In order to test these possibilities, we knocked down *myoID* by RNAi specifically in the A8 segment (using *Abd-B^{LDN}-Gal4*, hereinafter referred to as *A8-GAL4*) or in the hindgut (using *hindgut-Gal4*) and looked at terminalia rotation and adult hindgut looping in both cases. *myoID* invalidation in the hindgut did not affect terminalia rotation but was sufficient to induce a sinistral and mislooped adult hindgut (Figure 1G); reciprocally, when *myoID* was specifically silenced in the A8 segment, the terminalia was misrotated but the hindgut properly looped (Figure 1G). These results show that (1) terminalia rotation and adult hindgut looping are two independent events and that (2) hindgut looping is controlled by a hindgut-specific MyoID-dependent organizer. Thus, we reveal that MyoID controls hindgut looping and terminalia rotation through two distinct tissue-specific organizers.

We next asked when MyoID activity is required for adult hindgut looping. Therefore, we knocked down *myoID* at different time periods during development using the Tub-Gal80ts/Gal4 system (TARGET method; McGuire et al., 2003). Using this approach, we show that *myoID* activity is required during days 3–5 of larval development for proper adult hindgut looping. Note that this functional time frame overlaps with the requirement of *myoID* activity during terminalia rotation (Figure 1H) (Petzoldt et al., 2012; Spéder et al., 2006), indicating that, although terminalia and



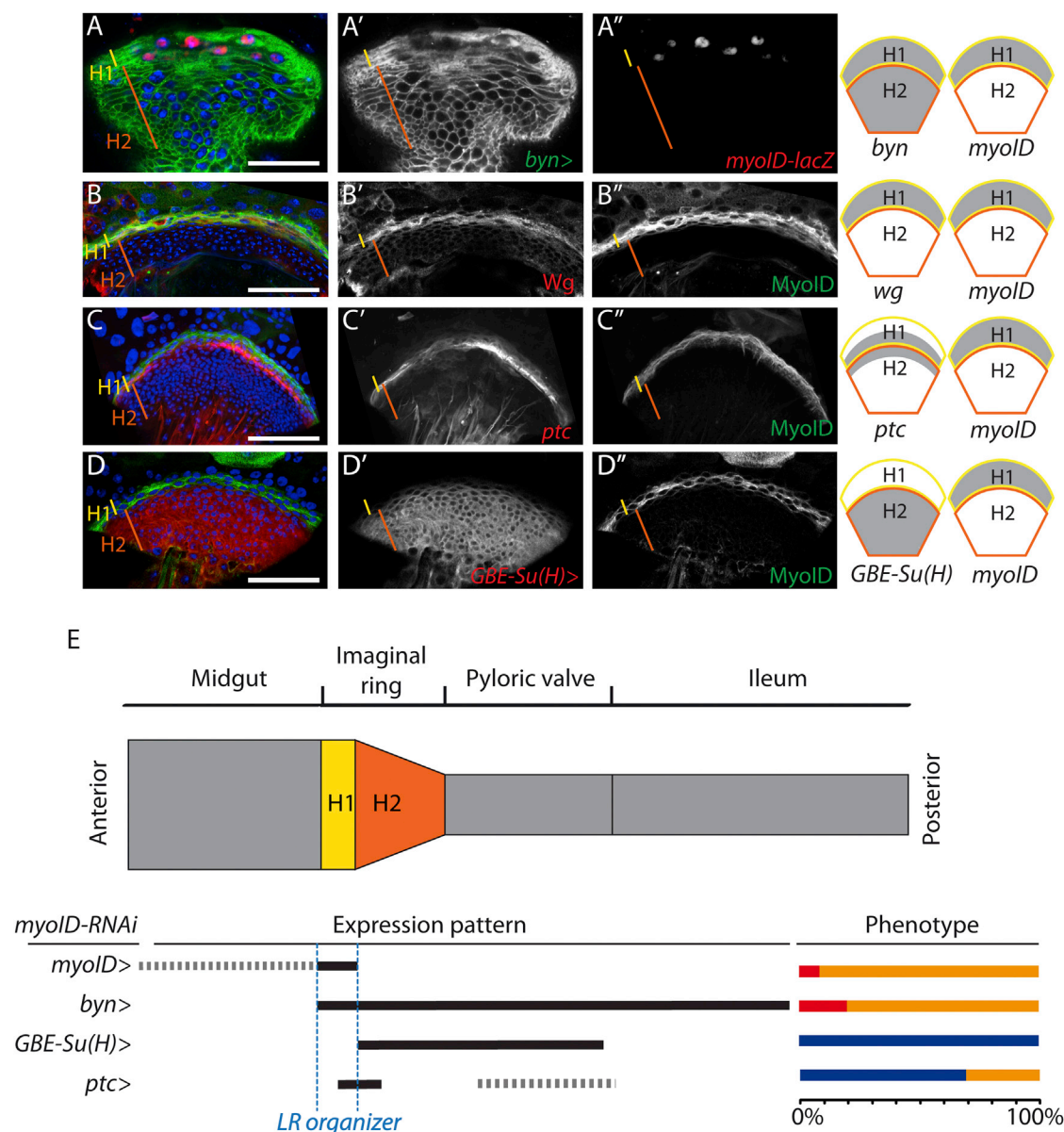


Figure 2. MyoD Is Expressed and Essential in the H1 Domain for Hindgut LR Asymmetry

(A–D'') Confocal images of L3 imaginal rings stained with specific markers expressed in the larval imaginal ring. Expression patterns shown in (A'–D') and (A''–D'') are schematized on the right in gray. MyoD is expressed specifically in the H1 domain, overlapping with Wg-expressing cells. The yellow and orange lines show positions for H1 cells and H2 cells, respectively. Scale bars, 50 μ m.

(E) Schematic representation of the larval digestive tract. The H1 (yellow) and H2 (orange) domains of the imaginal ring are shown. Summary of the phenotypes induced by *myoD* RNAi expression in the larval imaginal ring. Expression of MyoD specifically in the H1 domain is essential for proper dextral looping of the adult hindgut. Phenotypes are color coded as in Figure 1. See also Figures S1 and S2.

hindgut MyoD-dependent organizers are spatially distinct, they are temporally synchronous.

The Hindgut LR Organizer Lies in the H1 Domain of the Larval Imaginal Ring

As mentioned earlier, the adult hindgut derives from the larval imaginal ring that comprises two domains, a small anterior domain called H1 and a larger posterior domain called H2 (Fig-

ure 2E) (Murakami and Shiozaki, 2001). To precisely map MyoD-expressing cells in the imaginal ring, we analyzed the expression of several *myoD* reporter lines (*myoD*-Gal4, *myoD*-lacZ, and *myoD*::GFP) relative to that of known markers in the larval hindgut (*GBE-Su(H)*-Gal4, *hindgut*-Gal4; Figures 2A–2D; Figures S1A and S1B) (Fox and Spradling, 2009; Takashima et al., 2013) and *ptc*-Gal4 (described in this study; Figure 2C; Figures S1C and S1D). We found that MyoD-expressing

cells co-localize perfectly with Wg expression, which marks all H1 cells (Figure 2B). To check whether MyoID expression is exclusive of H1 cells, we used the posterior H1 and anterior H2 marker *ptc>GFP* (*ptc-Gal4*, *UAS-MCD8GFP*), which overlaps the H1-H2 boundary. Notably, MyoID colocalized with *ptc>GFP* in posterior H1 cells but not in H2 cells (Figure 2C; Figures S1C and S1D). These results were confirmed by checking the absence of MyoID expression from the H2 domain using an exclusive H2 marker (*GBE-Su(H)-Gal4*, *UAS-mCD8-GFP*) (Figure 2D; Figures S1A and S1B). From these data, we conclude that MyoID is precisely expressed in the H1 domain.

To test whether H1 cells may represent the adult hindgut LR organizer, *myoID* function was knocked down by RNAi using Gal4 drivers (Figure S1E) expressed in different portions of the ring domain. The sinistral phenotype observed using *myoID-Gal4* (H1 driver) was also obtained using *hindgut-Gal4*, which is expressed in both the H1 and H2 domains, and *ptc-Gal4*, which is expressed in a subset of posterior H1 cells as well as in anterior H2 cells (Figures 2A–2C and 2E). However, no phenotype was observed using the H2-specific driver (*GBE-Su(H)-Gal4*), indicating that H2 cells do not play a role in LR determination (Figures 2D and 2E), even though *GBE-Su(H)* is expressed at higher levels than *ptc-Gal4* or *myoID-gal4* (Figure S1E). In addition, the phenotype was not enhanced by combining H1 and H2 drivers (Figures S2A and S2B). Altogether, these data show that MyoID activity in the H1 domain is necessary and sufficient for proper LR asymmetry of the adult hindgut. Furthermore, these data show that the newly identified *Drosophila* MyoID-dependent LR organizer is localized in the H1 domain of the imaginal ring.

The Hindgut LR Organizer Is a Transient Structure

Although lineage-tracing experiments have identified the adult pylorus and ileum precursors, the exact contribution of the H1 domain to different parts of the tissue has not been revealed (Takashima et al., 2013). Therefore, we analyzed the contribution of H1/MyoID cells to the adult hindgut through a lineage-tracing method using the *myoID-Gal4* line (see Supplemental Experimental Procedures; lineage tracing using UAS-flipase and flipouts allows us to trace the lineage of cells expressing a specific Gal4 driver and, by gating Gal4 effectiveness with Gal80^{ts}, limits the tracing to those cells expressing Gal4 at the time of heat shock). We confirmed that the progeny of H1+H2 cells (*hindgut-Gal4* lineage) or H2 cells alone (*GBE-Su(H)-Gal4* lineage) covers the entire adult hindgut, including the recently identified posterior terminal midgut (Figures 3A and 3B) (Takashima et al., 2013). However, the progeny of H1 cells (*myoID-Gal4* lineage) does not cover any cell population of the adult hindgut or midgut, similar to a negative control lacking a Gal4 transgene (Figures 3C and 3D), suggesting that, in fact, the adult hindgut derives solely from H2 cells.

To further determine the fate of H1 cells, we followed their behavior during pupal development. Consistent with our lineage-tracing experiments, *myoID-Gal4* is not expressed in the developing hindgut during late pupal stages, indicating that H1 cells have indeed a distinct fate from that of H2 cells (Figure 3L). In fact, at 7 hr after puparium formation (APF), H1 cells (expressing both MyoID and *hindgut-Gal4*) start to adopt a migratory behavior (Figure 3E), and at 10 hr APF, they are physically sepa-

rated from the rest of the imaginal ring (Figures 3F and 3G). Then, at 24 hr APF, H1 cells are found in the pupal midgut (Figures 3I and 3J), a transient structure responsible for larval midgut degradation prior to its elimination in the meconium by young adults (Takashima et al., 2011). Consistently, H1 cells are also found in the meconium (Figures 3M and 3N), indicating that the H1 cells are degraded in the pupal midgut along with other transient larval tissues. Note that H1 domain detachment is normal in *myoID* null mutants, indicating that *myoID* does not have a role in this process (Figures 3H and 3K). Altogether, this analysis demonstrates that the H1 domain is a transient structure. Thus, we hypothesized that intervention of the H1 domain in hindgut asymmetry breaking occurs prior to H1 detachment.

To test this model, H1 cells were ablated at different time points by driving expression of the pro-apoptotic gene *reaper* in a temperature-dependent manner (using *myoID-Gal4; tub:Gal80^{ts}*). Strikingly, ablating the H1 domain between 0 and 10 hr APF resulted in a mislooped phenotype, whereas ablation of H1 after 10 hr APF (i.e., after H1 detachment) had no effect on adult hindgut looping. Notably, the overall adult hindgut integrity—and, in particular, the midgut-hindgut junction—was not compromised by H1 ablation, as shown by histochemical analysis and retention of blue food dye in adult guts (Figure S3). These results are consistent with the fact that H1 cells do not structurally constitute the adult hindgut and further demonstrate that the H1 domain is essential prior to detachment to control hindgut asymmetry.

Furthermore, our results redefine the adult hindgut fate map. Indeed, previous work has shown that the boundary between the hindgut and the midgut is not stable, with some anterior hindgut cells crossing the border to invade the midgut to form the posterior terminal midgut (Takashima et al., 2013). However, we show that the most anterior MyoID/Wg/H1 cells are eliminated and, thus, do not contribute to the posterior terminal midgut. Therefore, we propose that H2 cells are the adult hindgut proper primordial cells (with the most anterior H2 cells invading and constituting part of the midgut), whereas H1 cells are, in fact, transient, non-structural, regulatory cells that provide the LR directional cue guiding adult hindgut looping.

H1 Cells Transmit Directionality to the Hindgut Precursor Cells

Since the H1 domain detaches from the adult hindgut primordium well before hindgut looping and morphogenesis (approximately 50 hr before), it raises the question of how H1 MyoID-generated LR information is translated to H2 cells. Therefore, we analyzed cell behavior in the H2 domain during early pupal development. Cell shape changes and orientation were characterized by measuring the orientation of cellular membranes relative to the AP axis (Viktorinová and Dahmann, 2013) (Figures 4A and 4B; see Figures S4A, S4B, and S4G for details of the method). Before puparium formation (larval stage 3 [L3]), H2 cells are oriented perpendicularly to the AP axis, with no visible LR asymmetry (Figures 4C, 4F, and 4I). Strikingly though, the first visible cell shape changes occur at 10 hr APF, when H2 cells become oriented with a +50° bias relative to the AP axis; we call this orientation dextral by convention (Figures 4D, 4G, and 4J). Notably, H2 cells in *myoID* mutants are inverted compared to those in wild-type, showing an orientation of −50° (sinistral) (Figures 4E, 4H, and 4K). Measurement of cell orientation by

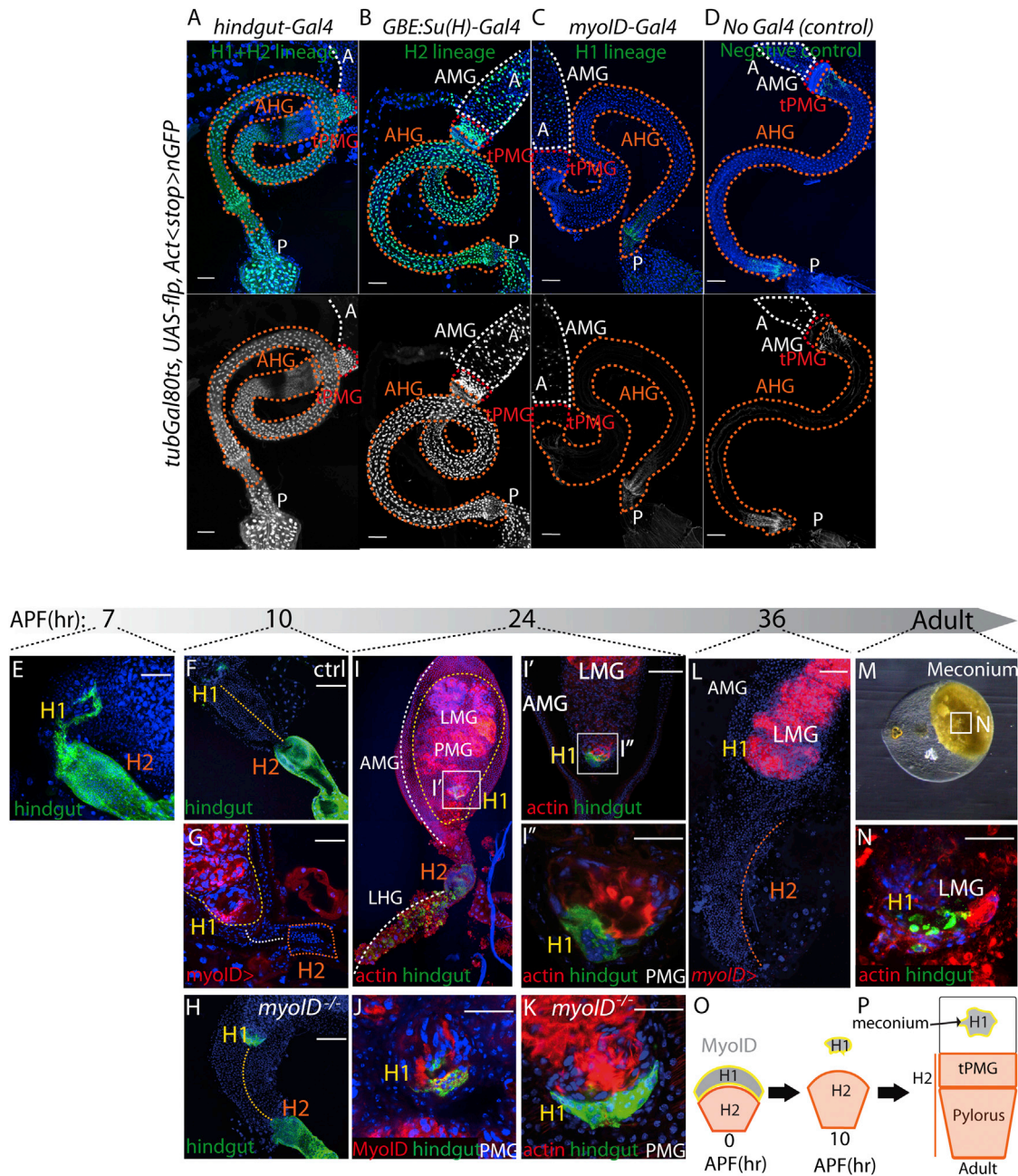


Figure 3. The Hindgut Organizer Is a Transient Structure

(A–D) Lineage-tracing experiments showing the progeny (GFP, green) of H1+H2 (A), H2 (B), or H1 (C) cells or a negative control (D). The green signal near the posterior end (P) of the hindgut in (C) and (D) corresponds to auto-fluorescence. Due to the large size of the hindgut, images were obtained by stitching multiple scans. AMG, adult midgut. AHG, adult hindgut, A, anterior. tPMG, terminal posterior midgut. N = 20 guts per genotype with 100% penetrance. Scale bars in all panels, 50 μ m.

(E) The H1 domain, marked by *hindgut-Gal4* starts to separate from the H2 domain around 7 hr APF.

(F) Detachment of the H1 domain is complete at 10 hr APF. The yellow dashed line shows the distance between H1 and H2 cells.

(G) *myoD-Gal4* expression is no longer seen in the hindgut (orange dotted line) starting at 10 hr APF.

(H) Similar to (F), detachment of H1 is not impaired in *myoD* mutants.

(I–I'') At 24 hr APF, H1 cells (expressing GFP) are trapped inside the pupal midgut (PMG, encircled, yellow dashed line), together with the larval midgut (LMG); H2 cells, on the other hand, are located between the adult midgut (AMG) and the degrading larval hindgut (LHG, marked by white dashed lines). (I') and (I'') are magnification images from (I). Due to the large size of the hindgut, the image was obtained by stitching multiple scans.

(J) At 24 hr APF, H1 cells present in the pupal midgut still express *myoD::GFP* (red) and *hindgut-Gal4* (green).

(K) At 24 hr APF, *myoD* mutants H1 cells, marked with *hindgut-Gal4*, are also trapped in the pupal midgut.

(L) At 36 hr APF, *MyoD* expression is not detectable in H2 cells (orange line).

(legend continued on next page)

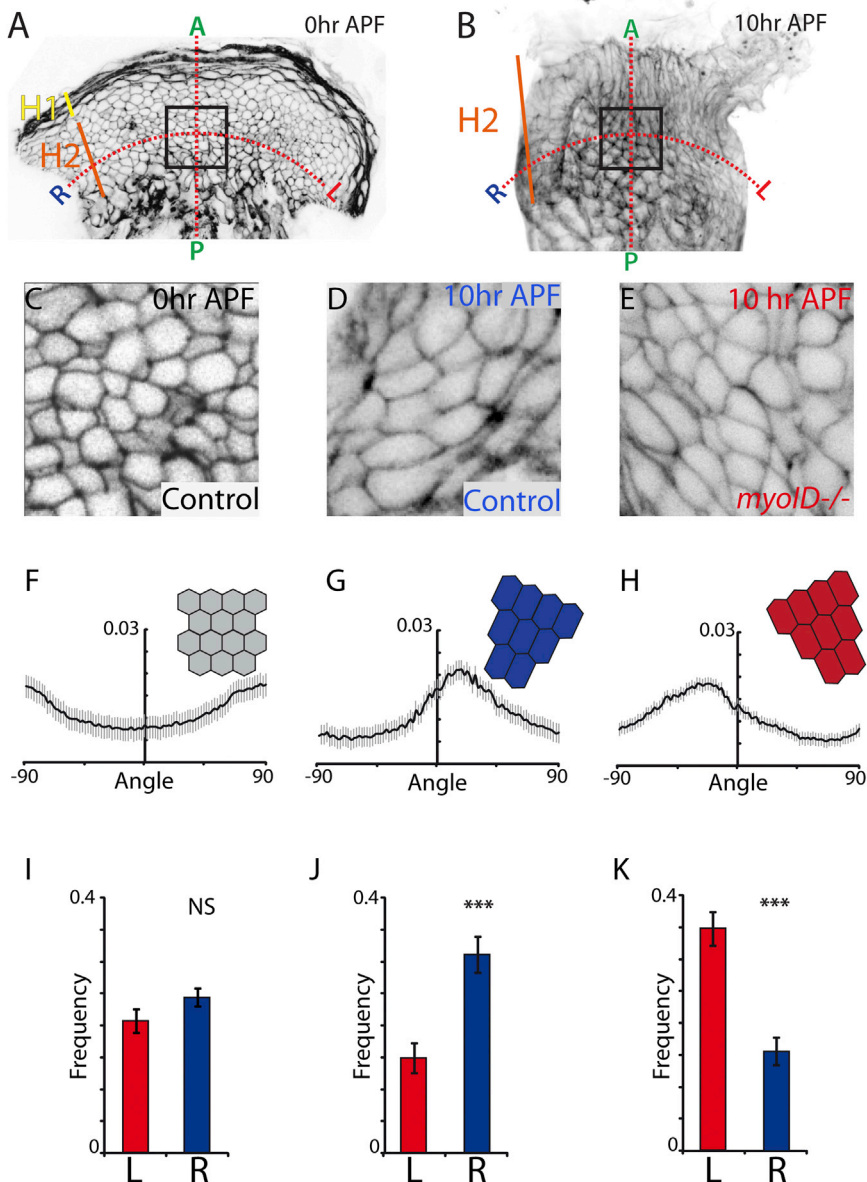


Figure 4. MyoID Controls Early LR Polarization of H2 Cells

(A and B) Representative L3 (A) and 10 hr APF (B) imaginal rings expressing *PH::GFP* to mark cell membranes (*hindgut-Gal4*, *UAS-PH::GFP*). The black box delineates the region used for quantitative measurements. R, right; L, left; A, anterior; P, posterior.

(C–E) Representative images of H2 cells at different time points. At 0 hr APF, cells do not show any LR bias (C), whereas at 10 hr APF, cells become elongated and orient toward the right side (D). In *myoID* null mutants, cells show an inverted orientation toward the left side (E).

(F–H) Graphic plot showing the distribution of cellular angles found in H2 cells at 0 hr APF in wild-type cells (control, F) and at 10 hr APF in wild-type (G) and *myoID* mutant cells (H). Mean values are represented by a solid line, and SEM is shown in gray. In (F), the peak at 90°/–90° represents symmetrical orientation along the hindgut AP axis, whereas in (G) and (H), peaks indicate preferential rightward or leftward orientations measured at 10 hr APF. N = 10 guts for each genotype.

(I–K) Plot of the sum of rightward (R) against leftward (L)-oriented angles. At 0 hr APF, there is no significant LR preference (I), while at 10 hr APF, there is a clear 2.5-fold difference between R and L (J). In *myoID* mutants, this difference is inverted (K). Error bars indicate SE. ***p < 0.0001; NS, non-significant.

See also Figure S4.

an alternative method using cell long-axis led to the same conclusion (Figures S4A–S4F).

Altogether, these data indicate that MyoID activity in H1 cells orchestrates the early H2 cell-shape changes underlying directional looping of the adult hindgut. Thus, *myoID* has an instructive and cell-non-autonomous function in H1 to direct LR asymmetry of the H2 hindgut precursor cells.

PCP Mediates LR Polarity of H2 Cells

The question remains as to how LR asymmetry is transmitted and maintained in H2 cells from H1 detachment to looping

morphogenesis. It is noteworthy that cell-shape changes in H2 cells occur in the plane of the epithelium. Therefore, we asked whether the PCP pathways that set and maintain PCP in other epithelia (Axelrod, 2009; Goodrich and Strutt, 2011; Peng and Axelrod, 2012) are also required for hindgut LR polarity. To do so, we drove RNAi targeting components of the core and global PCP pathways in either H1 (*myoID-Gal4*) or H1+H2 cells (*hindgut-Gal4*). Knocking down any of the core system components in H1+H2 cells resulted in a penetrant mislooped adult hindgut phenotype (Figures 5B–5D and 5E; Figure S5A). In contrast, RNAi depletion solely in H1 cells did not lead to any looping defect (Figure 5F), suggesting that the core PCP genes are required in H2 cells alone for maintaining proper polarity and looping of the adult hindgut.

Similar to the core system, RNAi depletion of the global PCP pathway *ft*, *ds*, or *fj* genes in H1+H2 or H2 cells (using *hindgut-GAL4* or *GBE-Su(H)-Gal4*, respectively) resulted in a highly penetrant mislooped phenotype (Figures 5G–5I and 5K; Figures S5B

(M) The pupal midgut, together with the remnants of the larval midgut, is expelled during the first hours of adult life in the meconium.

(N) Confocal image of a meconium showing *hindgut-Gal4*-positive cells.

(O) Schematic representation of H1 domain behavior at different time points showing the detachment of the H1 domain from the H2 domain.

(P) Schematic representation of the fate map of adult hindgut and posterior midgut.

See also Figure S3.

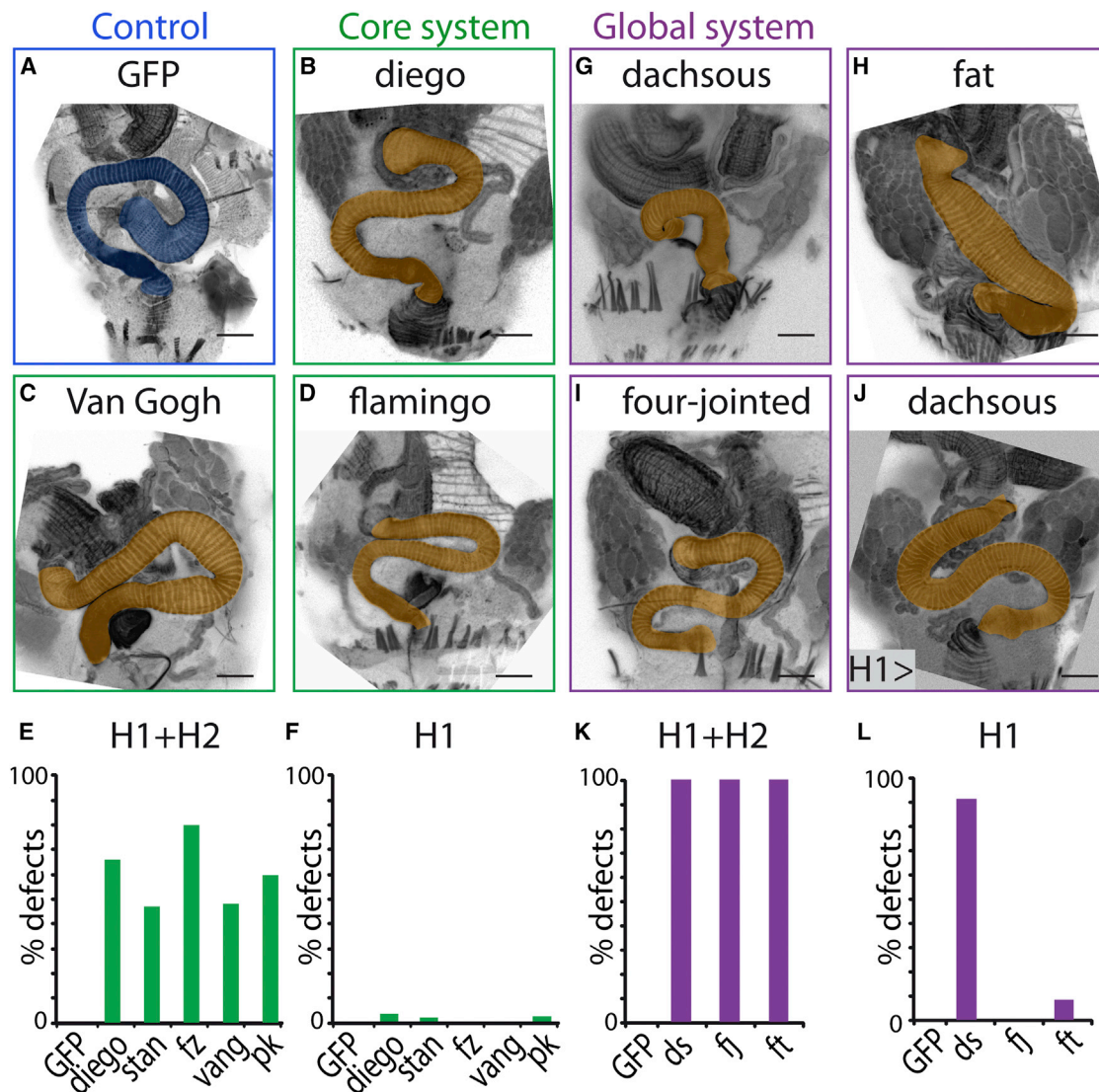


Figure 5. Hindgut Phenotypes of Core and Global PCP Genes

(A–D) and (G–J) show hindgut phenotypes from control flies (A), flies expressing RNAi against core (green, B–D) or global (purple, G–J) PCP pathway genes, and flies expressing *ds-RNAi* specifically in the H1 domain (J). Representative confocal images are shown with false-colored hindguts for clarity (color coded as in Figure 1). Scale bar, 100 μ m. In (E), (F), (K), and (L), histograms show the percentage of hindgut rotation defects following RNAi depletion of the core and global system components in the entire imaginal ring (H1+H2 domains), using *hindgut-Gal4* (E and K), or specifically in H1 cells, using *myoID-Gal4* (F and L). N = 100 for each genotype. See also Figures S2 and S5.

and S5D). Surprisingly though, and unlike for any other member of the PCP pathways, knockdown of *ds* specifically in H1 cells resulted in a highly penetrant mislooped phenotype, indicating that *ds* is essential in the H1 domain for adult hindgut asymmetry (Figures 5J and 5L; Figure S5C). Depletion of *fat* led to a weak phenotype, which could be enhanced by removing one copy of the gene (Figure 5L; Figure S2C). In contrast, *fj* loss of function did not show any phenotype (Figure 5L; Figure S2D), consistent with its expression being restricted to the posterior H2 region (Figures S2E–S2E’’’).

The strong *ds* loss-of-function phenotype reveals that Ds plays a non-autonomous role in H1 cells to direct H2 directionality. Altogether, these results indicate that adult hindgut looping

relies on proper PCP signaling in both H1 and H2 compartments. Although both Fz and Ft/Ds systems participate in maintaining LR orientation in H2 cells, the atypical cadherin Ds achieves a specific function in the H1 domain.

Ds Interacts with MyoID to Control Early LR Polarity of H2 Cells Non-Autonomously

To further assess the role of Ds in H1 cells, we specifically removed *ds* function from H1 cells using *myoID-Gal4* and analyzed H2 cell orientation. Notably, the quantification of membrane orientation showed a complete loss of H2 cell orientation bias (Figures 6A and 6B). Therefore, *ds* is essential in H1 cells for H2 cell LR polarity. Notably, the absence of bias inversion

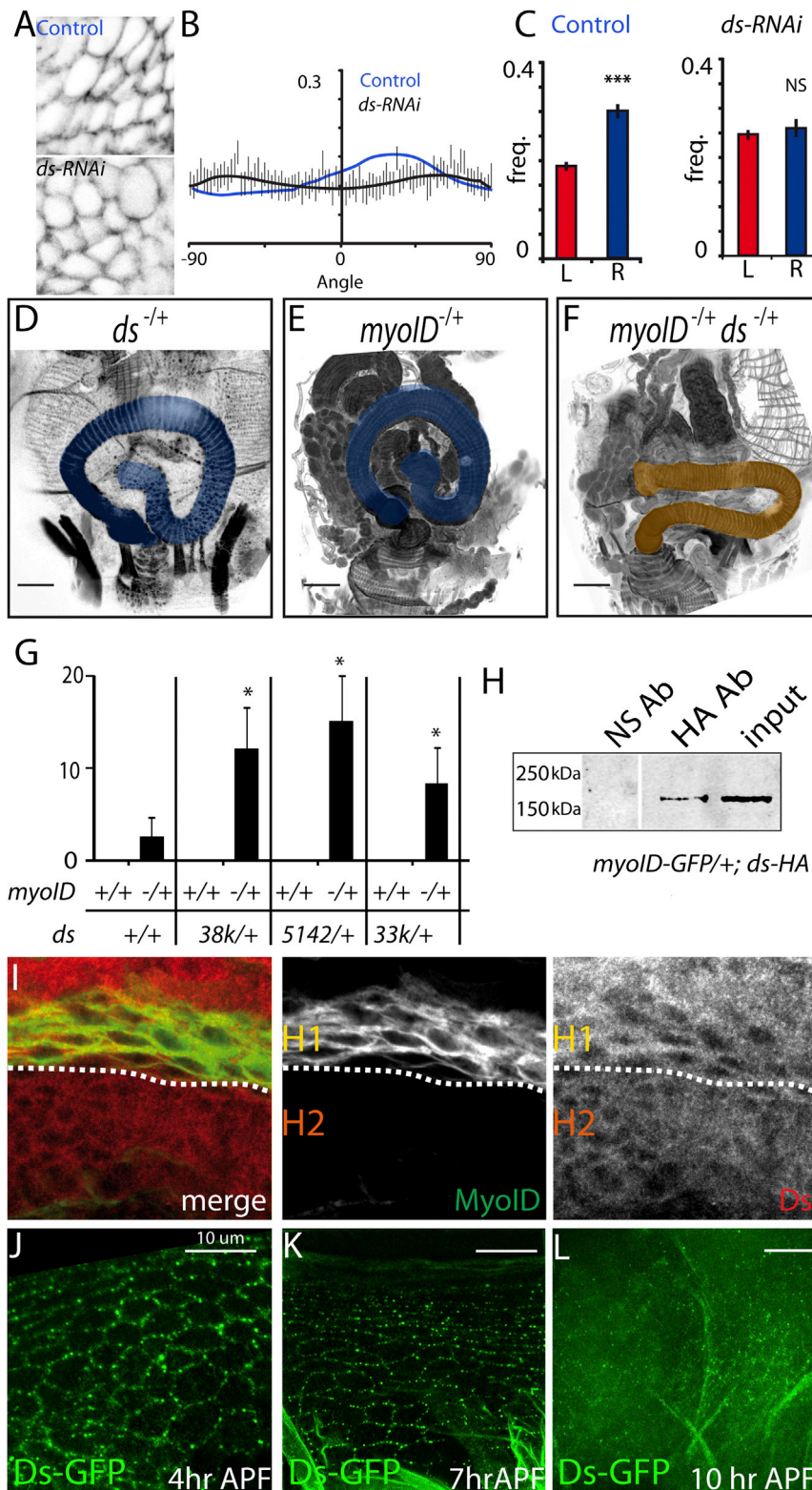


Figure 6. Genetic and Biochemical Interaction between MyoID and Ds in H1 Cells

(A) Representative images of H2 cells at 10 hr APF, from control flies (top) or *ds-RNAi* flies (bottom). Cells are elongated and oriented toward the right side in control, while in *ds-RNAi* flies, cells do not show any bias as in early 0 hr APF H2 cells (compare with Figure 4C).

(B) Knockdown of *ds* in the H1 domain results in a loss of LR polarity as revealed by the distribution of cellular angles found in H2 cells compared to the control (blue line). $N = 10$ guts for each genotype. (C) Plot of the sum of rightward (R)- and leftward (L)-oriented angles after depletion of Ds in H1 cells at 10 hr APF. Control cells show a bias toward the right side, while depletion of *ds* from H1 cells leads to a loss of the LR bias. Error bars indicate SE. *** $p < 0.0001$; NS, non-significant.

(D–F) Phenotype of heterozygous *ds* (D), *myoID* (E), or double *ds*; *myoID* heterozygote (F) flies. Representative confocal images are shown with false-colored hindguts for clarity (color coded as in Figure 1). $N = 100$ guts for each genotype. Scale bars, 100 μ m.

(G) Histogram showing the percentage of defects in single and double heterozygous flies mutant for *ds* and/or *myoID*. Error bars indicate SE. * $p < 0.01$. $N = 100$ for each genotype.

(H) Co-immunoprecipitation experiment using *myoID-gal4*, *UAS-myoID::GFP*; *atpB-P(acman-ds::HA)* larval hindgut extracts. MyoID is specifically immunoprecipitated by Ds::HA but not if a non-specific antibody is used (NS Ab).

(I) Confocal image of an imaginal ring from a larva overexpressing MyoID::GFP and Ds-HA at low levels (*myoID-Gal4*, *UAS-myoID::GFP*; *atpB-P(acman-ds::HA)*). Ds expression is visible in both H1 (marked by *myoID-Gal4*) and H2 cells. White dashed line outlines the H1/H2 border.

(J–L) Confocal images of *Ds-GFP* knockin allele showing Ds membrane distribution at 4 hr APF (J), 7 hr APF (K), and 10 hr APF (L).

See also Figure S6.

guidance cannot be conveyed to H2 cells; thus, the tissue remains naive.

The unique involvement of Ds in the H1 domain suggests a possible interaction with MyoID to direct LR asymmetry. To test this hypothesis, we evaluated potential genetic interactions between the two genes. Heterozygous mutant flies for *ds* or *myoID* show mislooped phenotypes with no or very low penetrance (~2%), respectively (Figures 6C and 6D). However, in double-heterozygous flies mutant for one *myoID* and one *ds* allele, the frequency of mislooped defects is significantly raised (Figures 6E and 6F), indicating that

in *ds* mutants, as observed in *myoID* mutant conditions, indicates that *ds* is essential in H1 to transmit both dextral and sinistral orientations. Therefore, in the absence of *ds*, directional

myoID and *ds* interact for proper adult hindgut looping and suggesting they affect a common process important for LR asymmetry.

Ds Intracellular Domain Is Responsible for MyoID-Dependent LR Polarization

Previously, MyoID has been shown to bind β -catenin and *Drosophila* E-cadherin (DE-cadherin) for proper looping of the terminalia (Petzoldt et al., 2012; Taniguchi et al., 2011). Since Ds is an atypical cadherin whose expression is needed in the same domain as MyoID in the imaginal ring (Figure 5), we tested whether MyoID and Ds also interact molecularly. For this purpose, we expressed both MyoID-GFP- and Ds-hemagglutinin (HA)-tagged proteins in the H1 domain. In this experiment, a genomic construct for Ds (*Ds::HA*) and *myoID-Gal4* was used to drive tagged proteins (Figure 6I). Co-immunoprecipitation with anti-HA antibodies from larval hindgut extracts led to the specific pulldown of MyoID::GFP (Figure 6H; specificity of the anti-HA immunoprecipitation was tested in a separate experiment and did not show any cross-reaction; Figure S6). These data show that MyoID and Ds bind in a same complex and interact together in H1 cells for proper LR morphogenesis of the hindgut.

MyoID is known to act inside cells; therefore, we checked whether MyoID specifically interacts with the Ds intracellular domain (ICD). Tagged forms of MyoID (MyoID-GFP) and the Ds intracellular domain (Ds amino acids 3120–3556; Ds-ICD-Flag) were co-expressed in *Drosophila* S2R+ cells. It is interesting that we noticed that both proteins co-localize and accumulate at membrane sites in contact with neighboring cells (Figure 7A). This co-localization was further supported biochemically in a co-immunoprecipitation assay showing that MyoID-GFP is able to co-immunoprecipitate the full-length intracellular domain of Ds (Figure 7B).

In other planar polarized epithelia, *ds* overexpression induces long-range polarity rearrangements due to Ds protein mislocalization (Ambegaonkar et al., 2012; Brittle et al., 2012; Bosveld et al., 2012; Matakatsu and Blair, 2006). Notably, overexpression of *ds* in H1 cells induces a gain-of-function mislooped phenotype in about 40% of flies (Figure 7D), suggesting that stoichiometry between MyoID and Ds should be maintained in H1 cells. Thus, overexpression of MyoID would be expected to, at least partially, rescue the *ds* overexpression phenotype. In fact, the *ds* overexpression phenotype (but not the *fat* overexpression phenotype; Figure S2F) was fully rescued by co-overexpression of *myoID* in H1 cells (Figures 7G and 7J), corroborating the importance of the Ds-MyoID interaction in H1 for proper looping. To further test the MyoID/Ds interaction, we performed epistasis experiments in H1 cells. When *ds* is overexpressed in H1 cells along with an RNAi against *myoID*, all hindguts are mislooped and none show sinistral looping (Figure S2G). In addition, depletion of both *ds* and *myoID* also lead to a mislooped phenotype (Figure S2H). Although some alternative models of interaction may take place, these results suggest that *ds* lies downstream of *myoID* to set LR asymmetry of the hindgut.

We used the rescue assay described earlier to further probe which of the Ds domains is required for interaction with MyoID in vivo by overexpressing truncated forms of Ds, lacking either the intracellular (*ds Δ ICD*) or the extracellular (*ds Δ ECD*) domain (Matakatsu and Blair, 2006). Expression of these truncated forms also led to a gain-of-function mislooped phenotype (Figures 7E and 7F). However, the phenotype induced by overexpression of *ds Δ ICD* was not at all rescued upon co-expression of MyoID

(Figures 7H and 7K), confirming that the Ds intracellular domain is, indeed, important for the interaction with MyoID. The mislooped phenotype observed by overexpression of *ds Δ ECD* is likely due to the displacement of endogenous full-length Ds/MyoID complexes or the production of abnormal Ds dimers (Figure 7F). Indeed, *ds Δ ECD* cannot bind to Ft; therefore, it cannot propagate planar polarity to other cells. Consistently, this phenotype was rescued by MyoID co-overexpression, which likely re-equilibrates the dose of active versus inactive complexes (Figures 7I and 7L).

Altogether, these results suggest that Ds/MyoID stoichiometry is important in vivo and that MyoID in H1 cells propagates LR asymmetry to H2 target cells through interaction with the intracellular domain of Ds in H1 cells.

DISCUSSION

In this work, we reveal the existence of an hindgut-specific LR organizer having transient activity. We show that LR information is transferred non-autonomously from this organizing center to the target tissue, involving a unique MyoID-Ds interaction taking place at a PCP signaling boundary (the H1/H2 boundary). Propagation of this initial LR information to the developing hindgut requires both Ds/Ft global and core Fz PCP signaling. Notably, these results suggest that MyoID can act as a directional cue to bias planar cell polarity.

So far, only a role for the core PCP pathway in cilia positioning and LR asymmetry had been reported in mouse, chick, and *Xenopus* (Zhang and Levin, 2009; Antic et al., 2010; Song et al., 2010). Here, we reveal a role of the Fat/Ds PCP pathway in LR asymmetry. We show that the atypical cadherin Ds is essential for early LR planar polarization of hindgut precursors and later on for looping morphogenesis. Ds has a cell-non-autonomous function, allowing transfer of LR information from the H1 domain to H2 hindgut precursor cells. Ds, therefore, represents a critical relay factor acting at the boundary between, and linking, a LR organizer and its target tissue.

In addition to a MyoID-dependent function in H1, the mislooped phenotype induced upon Ds silencing in the H2 domain (Figure 5; Figure S5D) suggests that Ds also has a MyoID-independent activity in H2 cells, likely through interaction with other PCP genes. Indeed, reducing the activity of PCP global or core gene functions reveals that the two pathways are important in the H2 region for adult hindgut looping (Figures S5D and S5E). However, the results reveal important differences in the way these pathways control hindgut asymmetry. First, although the adult phenotype is similar upon silencing of one or the other pathway, the early polarization of H2 cells in pupae (10 hr APF) is only affected when knocking down the activity of Ds, Ft, and Fz (Figure 5; data not shown). These results show that the Ds/Ft pathway, but not the core pathway, is required for establishing early LR polarity. Second, the phenotype is quantitatively different, since silencing of the *Ds*, *Ft*, or *Fz* PCP gene led to a consistent and very strong phenotype, while reducing Fz PCP signaling had a significantly less penetrant one. These data suggest a partly overlapping function of both PCP signaling pathways for late hindgut morphogenesis (Figure 5). Therefore, we propose the following sequential model (Figure 7M): in H1 cells, MyoID interacts with the Ds intracellular domain, which becomes

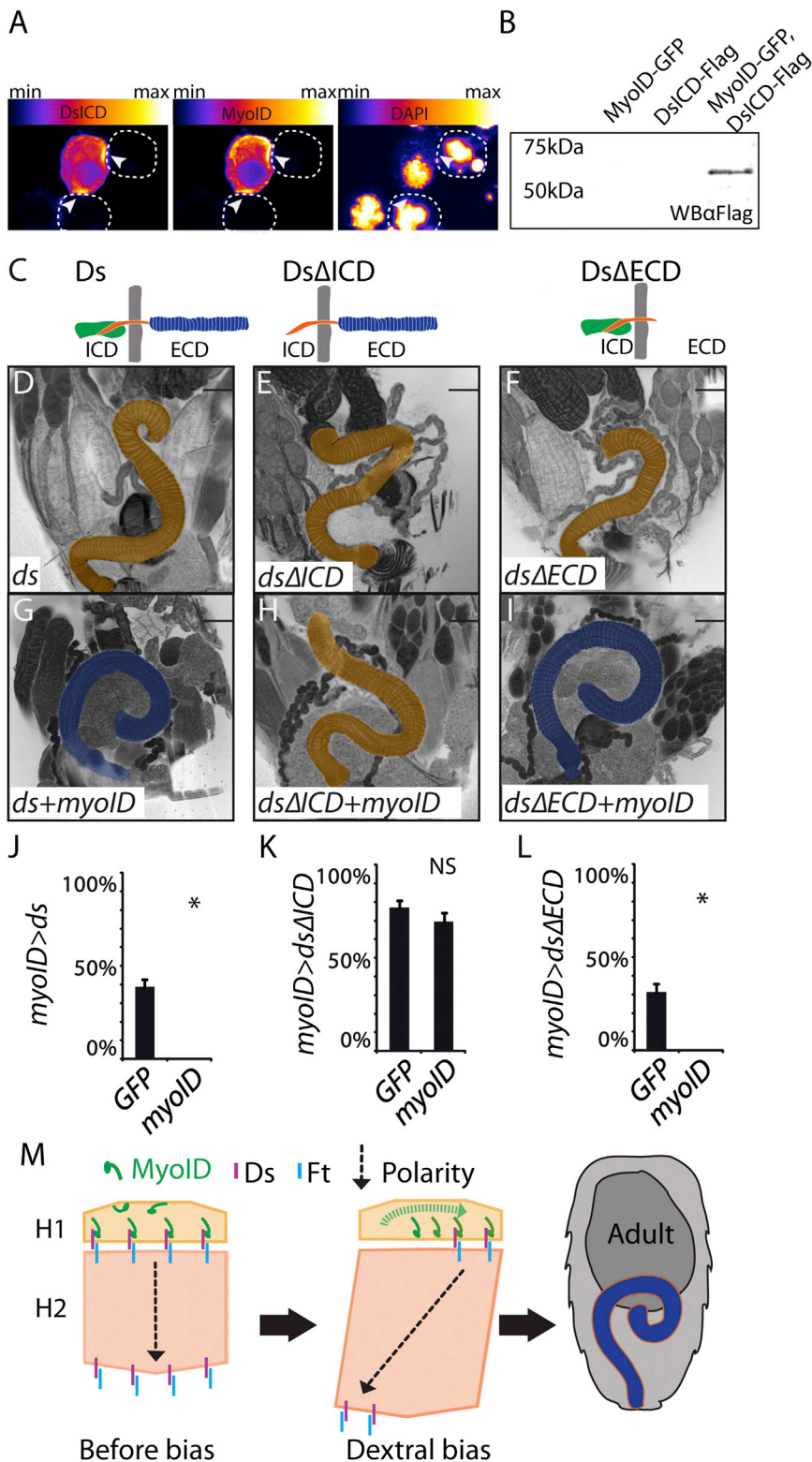


Figure 7. MyoID Interacts with Ds Intracellular Domain

(A) Co-expression of Ds-ICD and MyoID in *Drosophila* S2R+ cells reveals co-localization of both proteins at cell-cell contact sites (arrow-heads). Heatmap false-colored confocal images show protein concentration.

(B) Co-immunoprecipitation of Ds-ICD-Flag using MyoID::GFP as bait in *Drosophila* S2R+ cells.

(C) Cartoon of full-length and truncated forms of Ds used in (D–L), showing the intracellular domain (ICD, green), the transmembrane domain (orange), and the extracellular domain (ECD, blue).

(D–I) Hindgut phenotype from flies overexpressing different forms of Ds alone (D–F) or co-overexpressing different forms of Ds and MyoID (G–I). Scale bars, 100 μ m.

(J–L) Histogram showing the percentage of defects shown in (D)–(I). Error bars indicate SE. * $p < 0.01$. $N = 100$ for each genotype.

(M) Model of MyoID and Ds interaction in the H1 LR organizer. MyoID induces an “LR bias” (green dotted arrow) on Ds in H1 cells (represented by Ds localization on the right). This LR bias is then transferred to H2 cells through Ds/Ft interaction at the H1/H2 boundary. At 10 hr APF, H2 cells become polarized along the LR axis, initiating looping morphogenesis leading to a fully looped hindgut at 50 hr APF.

See also [Figure S2](#).

to the remaining H2 cells through classical Ds/Ft PCP. It is interesting that the local signaling boundary suggested by our model is consistent with recent studies showing that Ds can propagate polarity information in a range of up to eight cells, a distance that is consistent with the size of the H2 domain at 10 hr APF ([Figure 4](#)) ([Ambegaonkar et al., 2012](#); [Bosveld et al., 2012](#); [Brittle et al., 2012](#)). Once initial polarity has been set up through the Ds/Ft pathway, this is further relayed to and/or amplified by the core pathway. Notably, a similar two-step mechanism has also been proposed for the wing ([Hogan et al., 2011](#); [Ma et al., 2003](#); [Yang et al., 2002](#)) and could apply to other tissues ([Olofsson et al., 2014](#); [Ayukawa et al., 2014](#)).

The discovery of a coupling between the MyoID dextral factor and Ds is a nice example of crosstalk between existing signaling modules ([Noselli and Perri-mon, 2000](#)). In the simplest crosstalk model, the role of MyoID would just be to bias or tilt Ds function toward one

“biased” toward dextral through a currently unknown mechanism (discussed later). This initial LR bias is then transmitted across the H1/H2 boundary through Ds/Ft heterophilic interaction. Then, boundary H2 cells relay the initial bias and spread it

side, possibly through Ds localization and/or activity polarization along the LR axis ([Figure 7M](#)). Using both in vitro and in vivo assays, we show that interaction between Ds and MyoID requires Ds intracellular domain, supporting a cytoplasmic interaction

between the two proteins. These results, along with recent findings, suggest that Ds may represent a general platform for myosin function in different tissues. In particular, the intracellular domain of Ds was found to bind to the unconventional myosin Dachs, controlling Dachs polarized localization, which is important for subsequent cell rearrangements underlying thorax morphogenesis (Bosveld et al., 2012). However, in contrast to thoracic Dachs, MyoID is not obviously polarized in H1 cells (Figure 6), suggesting that the interaction between myosins and Ds may involve different mechanisms. Additionally, we could not detect any LR polarized localization of MyoID or Ds in H1 cells (Figures 6I–6L), although we cannot exclude the existence of subtle asymmetries undetectable by available tools. Nevertheless, alternative means to generate the LR bias in H1 include: (1) LR polarized expression of an unknown asymmetric factor or (2) LR asymmetric activity of Ds. These interesting possibilities are consistent with recent work showing that some type I myosins can generate directed spiral movement of actin filaments in vitro (Pyrpassopoulos et al., 2012). It is tempting to speculate that, similarly, MyoID putative chiral activity could be translated into Ds asymmetrical function along the LR axis (Figure 7M). Future work will explore this possibility as well as others to unravel the molecular basis of MyoID LR biasing activity in the H1 organizer.

The identification of the H1 domain as a specific adult tissue LR organizer demonstrates the existence of multiple independent tissue and stage-specific LR organizers in flies. This situation echoes what is known in other models, including vertebrates, in which at least two phases of asymmetry establishment can be distinguished. A first pre-gastrula phase, as early as the four-cell stage in *Xenopus*, involves the generation of asymmetric gradients of ions. Then, a second phase takes place at gastrulation and involves Nodal flow and asymmetric cell migration, eventually leading to asymmetric expression of the *nodal* gene in the left lateral plate mesoderm (Adams et al., 2006; Levin et al., 2002; Raya and Izpisua Belmonte, 2006). In *Drosophila*, some interesting common and specific features can be drawn out by comparing the hindgut and terminalia organizers (Géminard et al., 2014; Spéder et al., 2006). The first major common feature is the fact that both organizers rely on MyoID function, showing the conserved role of this factor in *Drosophila* LR asymmetry. Second, the two organizers show temporal disconnection, acting much earlier than LR morphogenesis, which is expected of a structure providing directionality to tissues per se (24 hr for terminalia and ~72 hr for hindgut looping). Such temporal disconnection of MyoID function with late morphogenesis is also observed in the terminalia where a peak of MyoID activity precedes terminalia rotation by 24 hr (Spéder et al., 2006; Suzanne et al., 2010). Time lag in MyoID function requires LR cue transmission and maintenance in developing tissues until directional morphogenesis. The finding of a role of Ds and PCP in hindgut LR asymmetry provides a simple mechanism by which initial LR information is maintained and transmitted across tissue through long-range PCP self-propagation.

Notably, the two organizers also show distinct features. In terminalia, MyoID has a cell-autonomous function in two adjacent domains (Suzanne et al., 2010). In addition, the terminalia organizer is permanent, developing as an integral component of the

adult tissue. In contrast, MyoID in the imaginal ring has a cell-non-autonomous function. Indeed, a striking feature of the hindgut organizer is its transience as it detaches from the hindgut precursors 50 hr before full looping morphogenesis prior to its degradation and elimination; hence, the need to transfer LR information to the H2 hindgut primordium. An interesting question then is whether the MyoID-Ds/PCP interaction is conserved in terminalia. We have shown that terminalia rotation requires the activity of DE-cadherin; however, invalidation of the atypical cadherins Ds or Ft or core PCP signaling in the terminalia organizer did not affect asymmetry (Petzoldt et al., 2012). The fact that PCP does not have a general role in *Drosophila* LR asymmetry is not altogether surprising, as MyoID cell-autonomous function in terminalia and organizer persistence does not require that LR information be transferred to and stored in other parts of the tissue, as is the case in the hindgut. Therefore, despite conservation of the MyoID-dependent upstream dextral cue, significant differences in downstream morphogenetic pathways imply alternative cellular mechanisms controlling cue transmission and maintenance.

The LR signaling module, comprising the dextral determinant MyoID and the still-unknown sinistral determinant, can therefore be coupled to distinct morphogenetic modules, including PCP, as shown in this study. We suggest that coupling between LR asymmetry and PCP might be observed in processes requiring long-distance patterning of tissues and organ precursors, both in invertebrate and vertebrate models. Understanding organ LR morphogenesis clearly requires studying diverse and complementary models. In this context, the multiplicity of LR organizers discovered in *Drosophila* represents a powerful model to study the diversity in the coupling of LR organizers with downstream programs responsible for late tissue morphogenesis. In particular, the *Drosophila* hindgut represents an invaluable model for studying the genetic basis and molecular mechanisms coupling LR asymmetry with PCP patterning.

EXPERIMENTAL PROCEDURES

See Supplemental Experimental Procedures for details about the methods.

Genetics

The strain *w*¹¹¹⁸ was used as control. *TubP:Gal80^{ts}*, *UAS-FLP*, *Ubi-p63E(FRT-STOP)Stinger*, *ds*⁰⁵¹⁴², *ds*^{38k}, *ds*^{33k}, *fj*⁹⁻¹¹, *UAS:PH(γ)-GFP*, *UAS:myrRFP*, *10XStat92E-GFP*, *UAS:MCD8-GFP*, and *UAS:dicer2* were all obtained from the Bloomington *Drosophila* Stock Center (BDSC). The hindgut-specific *byn-Gal4* was originally described by Judith Ann Lengyel (Iwaki and Lengyel, 2002) but was given to us by Kenji Matsuno. The A8-specific *Abd-B^{LDN}-Gal4* was a gift from E. Sanchez Herrero (de Navas et al., 2006). *GBE-Su(H)-Gal4* drives expression in H2 cells and was a gift from Xiankun Zeng (Zeng et al., 2010). *ptc-Gal4*, *myoID-Gal4(NP1458)*, *myoID-lacZ*, *myoID^{K2/K2}*, *UAS:myoID-RNAi-2X*, and *UAS:myoID-GFP* have been previously described (Spéder et al., 2006). *P(w+, genomic-myoid-GFP)* is an insertion in the second chromosome that contains the genomic sequence of *myoID* in which a HA-GFP cassette has been placed before the stop codon and that can rescue *myoID^{K2/K2}* phenotypes. *attB-P(acman-ds-HA)* was a gift from Ken Irvine (Ambegaonkar et al., 2012). The *Ds::GFP* knockin allele was a gift from David Strutt (Brittle et al., 2012). The following RNAi lines were used: *ds*^{GD14350}, *ds*^{GD2646}, *ds*^{JM02842}, *ds*^{GD14350}, *fz*^{KK101190}, *fz*^{GD881}, *fz*^{JF03245}, *fz*^{GD430}, *fz*^{HMS01310}, *fz*^{JF02843}, *dgo*^{HMS01454}, *dgo*^{GD7575}, *dgo*^{KK109514}, *fz*^{GD4614}, *fz*^{KK108004}, *pk*^{GD1510}, *stan*^{HMS01464}, *stan*^{JF02047}, *stan*^{GD607}, *stan*^{GD1889}, *vang*^{GD1889}, *vang*^{KK108814}. They were obtained from the BDSC and Vienna *Drosophila* RNAi Center (VDRC).

TARGET System

Experiments were performed as described by Spéder et al. (2006) using the TARGET system (described in McGuire et al., 2003). In brief, synchronized fly populations of the genotype *myoD-Gal4*, *tub-Gal80TS/UAS-myoD-RNAi* were raised at 25°C (Gal4 OFF) and then moved for 1 day to 29°C (Gal4 ON). The same procedure was used in combination with *UAS-reaper* to genetically ablate H1 cells, but in this case, flies were kept at 29°C for 1 hr.

Lineage-Tracing Strategy

Flies carrying *myoD-Gal4* (H1), *GBE-Su(H)-Gal4* (H2), or *byn-Gal4* (H1-2) were crossed to flies bearing the following transgenes: *TubP:Gal80^{ts}*, *UAS-FLP*, and *Ubi-p63E(FRT.STOP)Stinger-GFP* (Evans et al., 2009). The offspring was raised at 18°C until larval stage 2 (L2) and then transferred and kept at 29°C to allow the expression of the *flp* gene, causing the excision of the stop cassette and leading to continuous Stinger-GFP expression. Finally, flies at the white prepupal stage were transferred back to 18°C to prevent further Stinger-GFP expression. Adults were dissected and analyzed for Stinger-GFP presence. As a negative control, both flies without a Gal4 construct and flies that never underwent the 29°C heat shock were used.

Antibodies and Staining

Larval and adult hindguts were dissected in PBS and fixed in 4% formaldehyde for 20 min. Subsequent washes and incubations were conducted in PBS with 0.1% Triton. Tissues were incubated overnight with primary antibody at 4°C, followed by a 2-hr incubation with secondary antibodies at room temperature. Antibodies used were mouse anti-Wg (Developmental Studies Hybridoma Bank [DSHB], 1:50) and mouse anti-B-Galactosidase (Promega 1:1,000). F-actin was stained using Phalloidin-Cy3-fluorescein isothiocyanate (FITC; Molecular Probes 1:400). FITC-, Cy3-, and Cy5-conjugated secondary antibodies were obtained from Jackson ImmunoResearch Laboratories and used at 1:200.

Blue Erioglaucine Staining

Flies were fed a mixture of 3% agar, 5% sucrose, and 2.5% erioglaucine (Sigma, #861146) for at least 6 hr. Then, the adult hindgut position was examined in a Leica MZ6 stereomicroscope.

Cell Polarity Measurements

A small square was selected in the middle of the H2 ring to minimize the effects of deformation caused by the architecture of a tube. Images were previously aligned along the AP axis. LR cell orientation was then analyzed with Fiji software, first manually by calculating the main axis of one cell and measuring its angle with the perpendicular AP axis and then by using the Fiji “Directionality” plug-in created by Jean-Yves Tinevez (<http://fiji.sc/directionality>). This plug-in gives the preferred orientation of structures present in the input image (cellular membrane) and plots them as a histogram of frequencies (Figure S4G).

For measuring the long-axis and cell orientation angle, cells were first segmented using the “find maxima” tool from Fiji with the “segmented particles” option as output. Finally, the segmented polygons were directly measured using the “measure tool” in Fiji software (Figures S4A–S4F).

SUPPLEMENTAL INFORMATION

Supplemental Information includes Supplemental Experimental Procedures and six figures and can be found with this article online at <http://dx.doi.org/10.1016/j.devcel.2015.04.026>.

ACKNOWLEDGMENTS

We thank J. Axelrod, Y. Bellaïche, S. Blair, S. Hou, K. Irvine, E. Sanchez-Herrero, D. Strutt, and G. Struhl for sharing reagents and fly lines; J.Y. Tinevez for help with the directionality plug-in; the TRiP facility at Harvard Medical School (NIH/NIGMSR01-GM084947), the BDSC, the VDRC, and the DSHB for reagents; the Institut de Biologie Valrose (IBV) PRISM imaging facility for advice and support; members of the laboratory for discussion and comments; and the anonymous reviewers for their valuable comments. N.G.-M. is supported by a CONACyT fellowship (288758 213221). Work in the S.N. laboratory is supported by CNRS, INSERM, the University of Nice, ANR, LABEX SIGNALIFE

(#ANR-11-LABX-0028-01), Fondation ARC, and Fondation pour la Recherche Médicale (FRM).

Received: July 17, 2014

Revised: February 4, 2015

Accepted: April 28, 2015

Published: June 11, 2015

REFERENCES

- Adams, D.S., Robinson, K.R., Fukumoto, T., Yuan, S., Albertson, R.C., Yelick, P., Kuo, L., McSweeney, M., and Levin, M. (2006). Early, H+-V-ATPase-dependent proton flux is necessary for consistent left-right patterning of non-mammalian vertebrates. *Development* 133, 1657–1671.
- Adler, P.N. (2012). The frizzled/stan pathway and planar cell polarity in the *Drosophila* wing. *Curr. Top. Dev. Biol.* 101, 1–31.
- Ambegaonkar, A.A., Pan, G., Mani, M., Feng, Y., and Irvine, K.D. (2012). Propagation of Dachsous-Fat planar cell polarity. *Curr. Biol.* 22, 1302–1308.
- Antic, D., Stubbs, J.L., Suyama, K., Kintner, C., Scott, M.P., and Axelrod, J.D. (2010). Planar cell polarity enables posterior localization of nodal cilia and left-right axis determination during mouse and *Xenopus* embryogenesis. *PLoS ONE* 5, e8999.
- Axelrod, J.D. (2009). Progress and challenges in understanding planar cell polarity signaling. *Semin. Cell Dev. Biol.* 20, 964–971.
- Ayukawa, T., Akiyama, M., Mummery-Widmer, J.L., Stoeger, T., Sasaki, J., Knoblich, J.A., Senoo, H., Sasaki, T., and Yamazaki, M. (2014). Dachsous-dependent asymmetric localization of spiny-legs determines planar cell polarity orientation in *Drosophila*. *Cell Rep.* 8, 610–621.
- Bastock, R., Strutt, H., and Strutt, D. (2003). Strabismus is asymmetrically localized and binds to Prickle and Dishevelled during *Drosophila* planar polarity patterning. *Development* 130, 3007–3014.
- Blum, M., Schweickert, A., Vick, P., Wright, C.V.E., and Danilchik, M.V. (2014). Symmetry breakage in the vertebrate embryo: when does it happen and how does it work? *Dev. Biol.* 393, 109–123.
- Bosveld, F., Bonnet, I., Guirao, B., Tili, S., Wang, Z., Petitalot, A., Marchand, R., Bardet, P.L., Marcq, P., Graner, F., and Bellaïche, Y. (2012). Mechanical control of morphogenesis by Fat/Dachsous/Four-jointed planar cell polarity pathway. *Science* 336, 724–727.
- Brittle, A., Thomas, C., and Strutt, D. (2012). Planar polarity specification through asymmetric subcellular localization of Fat and Dachsous. *Curr. Biol.* 22, 907–914.
- Casal, J., Struhl, G., and Lawrence, P.A. (2002). Developmental compartments and planar polarity in *Drosophila*. *Curr. Biol.* 12, 1189–1198.
- Coutelis, J.B., Petzoldt, A.G., Spéder, P., Suzanne, M., and Noselli, S. (2008). Left-right asymmetry in *Drosophila*. *Semin. Cell Dev. Biol.* 19, 252–262.
- Coutelis, J.-B., Géminard, C., Spéder, P., Suzanne, M., Petzoldt, A.G., and Noselli, S. (2013). *Drosophila* left/right asymmetry establishment is controlled by the Hox gene abdominal-B. *Dev. Cell* 24, 89–97.
- Coutelis, J.-B., González-Morales, N., Géminard, C., and Noselli, S. (2014). Diversity and convergence in the mechanisms establishing L/R asymmetry in metazoa. *EMBO Rep.* 15, 926–937.
- Cui, C., Little, C.D., and Rongish, B.J. (2009). Rotation of organizer tissue contributes to left-right asymmetry. *Anat. Rec. (Hoboken)* 292, 557–561.
- Das, G., Reynolds-Kennally, J., and Mlodzik, M. (2002). The atypical cadherin Flamingo links Frizzled and Notch signaling in planar polarity establishment in the *Drosophila* eye. *Dev. Cell* 2, 655–666.
- de Navas, L., Foronda, D., Suzanne, M., and Sanchez-Herrero, E. (2006). A simple and efficient method to identify replacements of P-lacZ by P-Gal4 lines allows obtaining Gal4 insertions in the bithorax complex of *Drosophila*. *Mech. Dev.* 123, 860–867.
- Evans, C.J., Olson, J.M., Ngo, K.T., Kim, E., Lee, N.E., Kuoy, E., Patananan, A.N., Sitz, D., Tran, P., Do, M.T., et al. (2009). G-TRACE: rapid Gal4-based cell lineage analysis in *Drosophila*. *Nat. Methods* 6, 603–605.

- Fox, D.T., and Spradling, A.C. (2009). The *Drosophila* hindgut lacks constitutively active adult stem cells but proliferates in response to tissue damage. *Cell Stem Cell* 5, 290–297.
- Fox, D.T., Gall, J.G., and Spradling, A.C. (2010). Error-prone polyploid mitosis during normal *Drosophila* development. *Genes Dev.* 24, 2294–2302.
- Géminard, C., González-Morales, N., Coutelis, J.-B., and Noselli, S. (2014). The myosin ID pathway and left-right asymmetry in *Drosophila*. *Genesis* 52, 471–480.
- Goodrich, L.V., and Strutt, D. (2011). Principles of planar polarity in animal development. *Development* 138, 1877–1892.
- Gray, R.S., Roszko, I., and Solnica-Krezel, L. (2011). Planar cell polarity: coordinating morphogenetic cell behaviors with embryonic polarity. *Dev. Cell* 21, 120–133.
- Gros, J., Feistel, K., Viebahn, C., Blum, M., and Tabin, C.J. (2009). Cell movements at Hensen's node establish left/right asymmetric gene expression in the chick. *Science* 324, 941–944.
- Hogan, J., Valentine, M., Cox, C., Doyle, K., and Collier, S. (2011). Two frizzled planar cell polarity signals in the *Drosophila* wing are differentially organized by the Fat/Dachsous pathway. *PLoS Genet.* 7, e1001305.
- Hozumi, S., Maeda, R., Taniguchi, K., Kanai, M., Shirakabe, S., Sasamura, T., Spéder, P., Noselli, S., Aigaki, T., Murakami, R., and Matsuno, K. (2006). An unconventional myosin in *Drosophila* reverses the default handedness in visceral organs. *Nature* 440, 798–802.
- Iwaki, D.D., and Lengyel, J.A. (2002). A Delta-Notch signaling border regulated by Engrailed/Invected repression specifies boundary cells in the *Drosophila* hindgut. *Mech. Dev.* 114, 71–84.
- Krasnow, R.E., Wong, L.L., and Adler, P.N. (1995). Dishevelled is a component of the frizzled signaling pathway in *Drosophila*. *Development* 121, 4095–4102.
- Lawrence, P.A., and Casal, J. (2013). The mechanisms of planar cell polarity, growth and the Hippo pathway: some known unknowns. *Dev. Biol.* 377, 1–8.
- Lawrence, P.A., Struhl, G., and Casal, J. (2007). Planar cell polarity: one or two pathways? *Nat. Rev. Genet.* 8, 555–563.
- Lenhart, K.F., Holtzman, N.G., Williams, J.R., and Burdine, R.D. (2013). Integration of nodal and BMP signals in the heart requires FoxH1 to create left-right differences in cell migration rates that direct cardiac asymmetry. *PLoS Genet.* 9, e1003109.
- Levin, M., Thorlin, T., Robinson, K.R., Nogi, T., and Mercola, M. (2002). Asymmetries in H⁺/K⁺-ATPase and cell membrane potentials comprise a very early step in left-right patterning. *Cell* 111, 77–89.
- Ma, D., Yang, C.H., McNeill, H., Simon, M.A., and Axelrod, J.D. (2003). Fidelity in planar cell polarity signalling. *Nature* 421, 543–547.
- Matakatsu, H., and Blair, S.S. (2004). Interactions between Fat and Dachsous and the regulation of planar cell polarity in the *Drosophila* wing. *Development* 131, 3785–3794.
- Matakatsu, H., and Blair, S.S. (2006). Separating the adhesive and signaling functions of the Fat and Dachsous protocadherins. *Development* 133, 2315–2324.
- Matis, M., and Axelrod, J.D. (2013). Regulation of PCP by the Fat signaling pathway. *Genes Dev.* 27, 2207–2220.
- McGuire, S.E., Le, P.T., Osborn, A.J., Matsumoto, K., and Davis, R.L. (2003). Spatiotemporal rescue of memory dysfunction in *Drosophila*. *Science* 302, 1765–1768.
- Mooseker, M.S., and Cheney, R.E. (1995). Unconventional myosins. *Annu. Rev. Cell Dev. Biol.* 11, 633–675.
- Morgan, N.S., Heintzelman, M.B., and Mooseker, M.S. (1995). Characterization of myosin-1A and myosin-1B, two unconventional myosins associated with the *Drosophila* brush border cytoskeleton. *Dev. Biol.* 172, 51–71.
- Morgan, D., Turnpenny, L., Goodship, J., Dai, W., Majumder, K., Matthews, L., Gardner, A., Schuster, G., Vien, L., Harrison, W., et al. (1998). Inversin, a novel gene in the vertebrate left-right axis pathway, is partially deleted in the inv mouse. *Nat. Genet.* 20, 149–156.
- Murakami, R., and Shiotsuki, Y. (2001). Ultrastructure of the hindgut of *Drosophila* larvae, with special reference to the domains identified by specific gene expression patterns. *J. Morphol.* 248, 144–150.
- Nakamura, T., and Hamada, H. (2012). Left-right patterning: conserved and divergent mechanisms. *Development* 139, 3257–3262.
- Namigai, E.K.O., Kenny, N.J., and Shimeld, S.M. (2014). Right across the tree of life: the evolution of left-right asymmetry in the Bilateria. *Genesis* 52, 458–470.
- Noselli, S., and Perrimon, N. (2000). Are there close encounters between signaling pathways? *Science* 290, 68–69.
- Olofsson, J., Sharp, K.A., Matis, M., Cho, B., and Axelrod, J.D. (2014). Prickle/spiny-legs isoforms control the polarity of the apical microtubule network in planar cell polarity. *Development* 141, 2866–2874.
- Peeters, H., and Devriendt, K. (2006). Human laterality disorders. *Eur. J. Med. Genet.* 49, 349–362.
- Peng, Y., and Axelrod, J.D. (2012). Asymmetric protein localization in planar cell polarity: mechanisms, puzzles, and challenges. *Curr. Top. Dev. Biol.* 101, 33–53.
- Petzoldt, A.G., Coutelis, J.B., Géminard, C., Spéder, P., Suzanne, M., Cerezo, D., and Noselli, S. (2012). DE-Cadherin regulates unconventional Myosin ID and Myosin IC in *Drosophila* left-right asymmetry establishment. *Development* 139, 1874–1884.
- Pyrpassopoulos, S., Feeser, E.A., Mazerik, J.N., Tyska, M.J., and Ostap, E.M. (2012). Membrane-bound myo1c powers asymmetric motility of actin filaments. *Curr. Biol.* 22, 1688–1692.
- Raya, A., and Izpisua Belmonte, J.C. (2006). Left-right asymmetry in the vertebrate embryo: from early information to higher-level integration. *Nat. Rev. Genet.* 7, 283–293.
- Robertson, C.W. (1936). The metamorphosis of *Drosophila melanogaster*, including an accurately timed account of the principal morphological changes. *J. Morphol.* 59, 351–399.
- Rogulja, D., Rauskolb, C., and Irvine, K.D. (2008). Morphogen control of wing growth through the Fat signaling pathway. *Dev. Cell* 15, 309–321.
- Sharma, P., and McNeill, H. (2013). Regulation of long-range planar cell polarity by Fat-Dachsous signaling. *Development* 140, 3869–3881.
- Simon, M.A., Xu, A., Ishikawa, H.O., and Irvine, K.D. (2010). Modulation of fat-dachsous binding by the cadherin domain kinase four-jointed. *Curr. Biol.* 20, 811–817.
- Singh, J., and Mlodzik, M. (2012). Planar cell polarity signaling: coordination of cellular orientation across tissues. *Wiley Interdiscip. Rev. Dev. Biol.* 1, 479–499.
- Song, H., Hu, J., Chen, W., Elliott, G., Andre, P., Gao, B., and Yang, Y. (2010). Planar cell polarity breaks bilateral symmetry by controlling ciliary positioning. *Nature* 466, 378–382.
- Spéder, P., Adám, G., and Noselli, S. (2006). Type ID unconventional myosin controls left-right asymmetry in *Drosophila*. *Nature* 440, 803–807.
- Suzanne, M., Petzoldt, A.G., Spéder, P., Coutelis, J.B., Steller, H., and Noselli, S. (2010). Coupling of apoptosis and L/R patterning controls stepwise organ looping. *Curr. Biol.* 20, 1773–1778.
- Takashima, S., Mkrtchyan, M., Younossi-Hartenstein, A., Merriam, J.R., and Hartenstein, V. (2008). The behaviour of *Drosophila* adult hindgut stem cells is controlled by Wnt and Hh signalling. *Nature* 454, 651–655.
- Takashima, S., Younossi-Hartenstein, A., Ortiz, P.A., and Hartenstein, V. (2011). A novel tissue in an established model system: the *Drosophila* pupal midgut. *Dev. Genes Evol.* 221, 69–81.
- Takashima, S., Paul, M., Aghajanian, P., Younossi-Hartenstein, A., and Hartenstein, V. (2013). Migration of *Drosophila* intestinal stem cells across organ boundaries. *Development* 140, 1903–1911.
- Taniguchi, K., Maeda, R., Ando, T., Okumura, T., Nakazawa, N., Hatori, R., Nakamura, M., Hozumi, S., Fujiwara, H., and Matsuno, K. (2011). Chirality in planar cell shape contributes to left-right asymmetric epithelial morphogenesis. *Science* 333, 339–341.

- Thomas, C., and Strutt, D. (2012). The roles of the cadherins Fat and Dachsous in planar polarity specification in *Drosophila*. *Dev. Dyn.* 241, 27–39.
- Tree, D.R.P., Shulman, J.M., Rousset, R., Scott, M.P., Gubb, D., and Axelrod, J.D. (2002). Prickle mediates feedback amplification to generate asymmetric planar cell polarity signaling. *Cell* 109, 371–381.
- Vandenberg, L.N., and Levin, M. (2013). A unified model for left-right asymmetry? Comparison and synthesis of molecular models of embryonic laterality. *Dev. Biol.* 379, 1–15.
- Viktorinová, I., and Dahmann, C. (2013). Microtubule polarity predicts direction of egg chamber rotation in *Drosophila*. *Curr. Biol.* 23, 1472–1477.
- Vinson, C.R., and Adler, P.N. (1987). Directional non-cell autonomy and the transmission of polarity information by the frizzled gene of *Drosophila*. *Nature* 329, 549–551.
- Wallingford, J.B. (2012). Planar cell polarity and the developmental control of cell behavior in vertebrate embryos. *Annu. Rev. Cell Dev. Biol.* 28, 627–653.
- Wolff, T., and Rubin, G.M. (1998). Strabismus, a novel gene that regulates tissue polarity and cell fate decisions in *Drosophila*. *Development* 125, 1149–1159.
- Yang, Y. (2012). Planar cell polarity during development. Preface. *Curr. Top. Dev. Biol.* 101, xi–xiii.
- Yang, C.H., Axelrod, J.D., and Simon, M.A. (2002). Regulation of Frizzled by fat-like cadherins during planar polarity signaling in the *Drosophila* compound eye. *Cell* 108, 675–688.
- Yoshida, S., and Hamada, H. (2014). Roles of cilia, fluid flow, and Ca²⁺ signaling in breaking of left-right symmetry. *Trends Genet.* 30, 10–17.
- Zeidler, M.P., Perrimon, N., and Strutt, D.I. (2000). Multiple roles for four-jointed in planar polarity and limb patterning. *Dev. Biol.* 228, 181–196.
- Zeng, X., Chauhan, C., and Hou, S.X. (2010). Characterization of midgut stem cell- and enteroblast-specific Gal4 lines in *Drosophila*. *Genesis* 48, 607–611.
- Zhang, Y., and Levin, M. (2009). Left-right asymmetry in the chick embryo requires core planar cell polarity protein Vangl2. *Genesis* 47, 719–728.